Molecular Conductors Based on *peri*-Ditellurium-Bridged Donors, 2,3-DMTTeA and TMTTeN

Emiko Fujiwara,[a] Hideki Fujiwara,[b] Bakhyt Zh. Narymbetov,[b] Hayao Kobayashi,[b] Masahiro Nakata,[a] Hajime Torii,[c] Akiko Kobayashi,*[a] Kazuo Takimiya,[d] Tetsuo Otsubo,[d] and Fumio Ogura[e]

Keywords: Tellurium / Conducting materials / Magnetic properties / Band structure

Molecular conductors based on *peri*-ditellurium-bridged polyacene donor molecules 3,4-dimethylanthra[1,9-*cd*:4,10-*c′d′*]bis[1,2]ditellurole (2,3-DMTTeA) and 2,3,6,7-tetramethylnaphtho[1,8-*cd*:4,5-*c′d′*]bis[1,2]ditellurole (TMTTeN) were prepared. The crystal structure analyses of neutral 2,3-DMTTeA molecule and its cation radical salts revealed that these crystals involve an orientational disorder of the asymmetrical molecule, 2,3-DMTTeA, and that the intermolecular network through tellurium atoms is very strong and dominant in terms of the construction of the crystal frameworks. In the crystal of $(TMTTeN)_2M(CN)_2$ (M = Ag and Au), the crystal structure analyses and the extended Hückel tight-binding band calculations indicated that these salts are quasi three-dimensional conductors. These salts are highly conductive (720–760 $S\,cm^{-1}$) and maintain metallic states down to about 50 K. Furthermore, the $Ag(CN)_2^-$ salt exhibited a Pauli paramagnetic behavior down to 2 K [χ(para) ≈ 2.0–2.5×10^{-4} $emu\,mol^{-1}$]. In the crystal of $(TMTTeN)(SCN)_{0.88}$, the donor molecules are stacked to form one-dimensional columns and construct a three-dimensional network between the columns through the intermolecular Te···Te contacts. The SCN^- salt is also highly conductive (590 $S\,cm^{-1}$) and maintains a metallic behavior down to 4.2 K. Almost temperature-independent paramagnetic susceptibility of $(TMTTeN)(SCN)_{0.88}$ indicates Pauli paramagnetism of this salt [χ(para) ≈ $1.6–1.9 \times 10^{-4}$ $emu\,mol^{-1}$]. A tight-binding band structure calculation indicates that the Fermi surface of the SCN^- salt is open along the b^* and c^* directions, but the intermolecular interactions between the donor columns are not so weak because of the three-dimensional network mediated by the protruded tellurium atoms.

Introduction

Over the past few decades, a considerable number of studies have been performed on the chemistry and physics of organic conductors.[1] The main principle of the molecular design of conductors with stable metallic states has been considered to be an achievement of the two-dimensional electronic state of molecular crystals that is realized by an introduction of sulfur and selenium atoms into π electron systems. These heavy chalcogen atoms included in π donor molecules are expected to increase the intermolecular interactions in the solid state and to yield wide conduction bands. In this sense, tellurium-containing molecular conductors are of special interest. However, very few attempts have been made on the tellurium-containing donor molecules,[2] such as tetratellurafulvalene (TTeF)[3] and hexamethylene-TTeF (HMTTeF),[4] because of difficulties of synthesis and poor solubilities to common organic solvents. Among them, crystal structures of $(HMTTeF)_4(PF_6)_2$ and $(HMTTeF)_2[Pt(dmit)_2]$,[5] where dmit is dimercaptoisotrithione, have been reported and revealed their unique donor arrangements. In addition, several years ago $(HMTTeF)(Et_2TCNQ)(THF)_x$ was reported to be metallic around room temperature, where Et_2TCNQ is 2,5-diethyl-7,7,8,8-tetracyano-*p*-quinodimethane.[6] However, no HMTTeF salt has been known to show a metallic behavior down to low temperatures. Therefore, no systematic research has been carried out thoroughly in terms of both the electrical conductivities and structure analyses of the HMTTeF salts. On the other hand, the TCNQ complex of TTeF showed a metallic behavior down to 2 K with a very high room temperature conductivity of 2200 $S\,cm^{-1}$ in comparison with those of its sulfur and selenium analogs.[7] This result indicates

[a] Research Centre for Spectrochemistry, School of Science, The University of Tokyo,
Hongo, Bunkyo-ku, Tokyo 113-0033, Japan
Fax: +81-3-5841-4417
E-mail: akiko@chem.s.u-tokyo.ac.jp
[b] Institute for Molecular Science,
Myodaiji, Okazaki 444-8585, Japan
[c] Department of Chemistry, School of Science, The University of Tokyo,
Hongo, Bunkyo-ku, Tokyo 113-0033, Japan
[d] Department of Applied Chemistry, Faculty of Engineering, Hiroshima University,
Kagamiyama, Higashi-Hiroshima 739-8527, Japan
[e] Department of Industrial Chemistry, Faculty of Engineering, Kinki University,
Umenobe-1, Takaya, Higashi-Hiroshima 739-2116, Japan

that organic metals possessing high conductivities and wide bandwidths can be realized by the substitution for tellurium atoms.

From the viewpoint of the crystal structures, furthermore, conducting salts based on tellurium-containing donors are interesting because the formation of a tellurium network seems to be dominant in terms of the construction of crystal structures. Polyacene donor molecules containing *peri*-ditellurium bridges are considered to utilize the atomic character of their protruded tellurium atoms more directly than the TTeF donors such as TTeF and HMTTeF. Needless to say, the tellurium crystal that has a three-dimensional Te···Te network shows a semimetallic behavior under ambient pressure and brings a superconducting transition at 3.3 K under pressure of 4.5 GPa,[8] which is extremely lower than the pressures required for a sulfur crystal (10.1 K under 93 GPa and 14 K under 157 GPa)[9] and a selenium crystal (6.8 K under 13 GPa).[10,11] Therefore, the tellurium-containing molecular conductors deserve much attention if such a nature of the tellurium crystal is reflected in their physical properties.

Tetratellurotetracene (TTeT)[12,13] is a well-known donor molecule containing *peri*-ditellurium bridges. However, few cation radical salts and charge transfer complexes of TTeT have been reported owing to its extremely poor solubility and their crystal structures have not been made clear so far.[14] Therefore, we focused on the other donors containing *peri*-ditellurium bridges such as 3,4-dimethylanthra-[1,9-*cd*:4,10-*c′d′*]bis[1,2]ditellurole (2,3-DMTTeA)[15] and 2,3,6,7-tetramethylnaphtho[1,8-*cd*:4,5-*c′d′*]bis[1,2]ditellurole (TMTTeN),[16] because their solubilities to organic solvents are considerably improved in comparison to other reported tellurium-containing donors because of the existence of methyl groups. We report here the structures of the neutral 2,3-DMTTeA and TMTTeN molecules, and the structures and physical properties of their cation radical salts.[17–19]

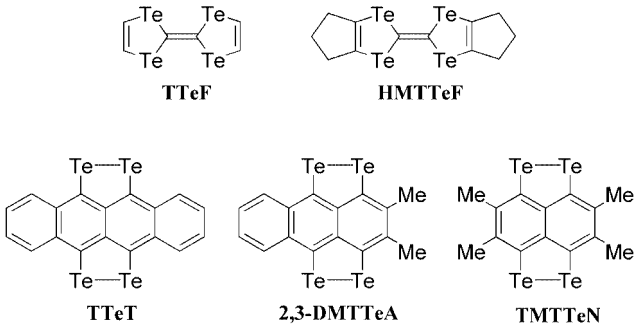

Results and Discussion

Molecular Structures and the Highest Occupied Molecular Orbital (HOMO)

In the early 1980s, we proposed to estimate the "dimensionality" of molecular conductors from their Fermi surfaces calculated by an extended Hückel tight-binding band approximation.[20] By virtue of the successful studies on low-temperature magnetotransport experiments of two-dimensional conductors around 1990,[21] the extended Hückel tight-binding band calculation was accepted as a conventional method to evaluate the dimensionality of electronic structures of organic conductors. Although sufficiently reliable empirical parameters of atomic orbitals that are used in the extended Hückel band calculations are hardly obtained even for selenium atoms, the accumulated information on the band structures of the organic conductors composed of selenium-containing tetrathiafulvalene (TTF)-like donors, such as tetramethyltetraselenafulvalene (TMTSF) and bis(ethylenedithio)tetraselenafulvalene (BETS), permits us fairly good band structure calculations. However, it is still not so clear whether a similar calculation could be applied to the tellurium-containing systems, especially to the conductors composed of non-TTF-type donors.

An ab initio molecular orbital (MO) calculation has been made on the TMTTeN molecule. The calculated HOMO has a π character as shown in Figure 1. Because the HOMO has an *anti*-bonding character at the Te–Te bond, the Te–Te bond length is expected to be shortened in its cationic state. As described later, the X-ray crystal structure analyses of TMTTeN systems with various formal charges of the molecules (δ) have been made. In Table 1, the formal charge (δ) dependence of the average bond lengths of $TMTTeN^{+\delta}$ molecules {δ = 0 (neutral crystal), 0.5 [the $Ag(CN)_2^-$ and $Au(CN)_2^-$ salts], 0.7 (the AsF_6^- salt) and 0.9 (the ClO_4^- and SCN^- salts)} is summarized (see also Figure 2).

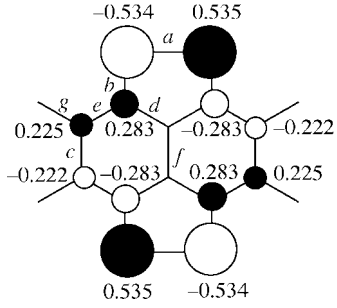

Figure 1. Schematic drawing of the HOMO of TMTTeN. Atomic orbital coefficients are also shown.

As shown in Figure 2, there seems to be a good correlation between δ and bond lengths in terms of the bonds *a* and *c* (see Figure 1, a). The shortening of the Te–Te (*a*) and C–C (*c*) bonds in the cationic state indicates the antibonding nature of the HOMO at these bonds, which is consistent with the result of the MO calculation. Thus, the HOMO will have an a_u symmetry with a node at the Te–Te bond. It is easily imagined that the node at the Te–Te bond is not favorable for the construction of molecular conductors with two- (or three-) dimensional electronic bands, despite the introduction of tellurium atoms. In contrast to the conductors based on TTF-like donors, whose HOMO has the same sign at every chalcogen atom, the transverse intermolecular interaction between TMTTeN molecules may be cancelled

Table 1. Bond lengths [Å] of TMTTeN. The bond lengths are averaged by assuming D_{2h} symmetry.[a]

	Neutral D[b]		$(D)_2Ag(CN)_2$	$(D)2Au(CN)^2$	$D(AsF_6)_{0.7}$	$D(SCN)_{0.88}$	$D(ClO_4)_{0.88}$
Formal charge (δ)	0		0.5	0.5	0.7	0.88	0.88
	Molecule A	Molecule B					
Te–Te (a)	2.7011(7)	2.6983(6)	2.664(1)	2.664(1)	2.666(2)	2.662(1)	2.666(3)
Te–C (b)	2.126(4)	2.218(4)	2.160(7)	2.113(8)	2.17(2)	2.113(8)	2.15(2)
C–C (c)	1.446(8)	1.427(8)	1.39(1)	1.41(2)	1.35(4)	1.39(1)	1.38(3)
C–C (d)	1.422(6)	1.429(5)	1.371(9)	1.42(1)	1.39(2)	1.410(7)	1.37(2)
C–C (e)	1.371(6)	1.387(6)	1.374(10)	1.38(1)	1.39(2)	1.400(7)	1.35(2)
C–C (f)	1.45(1)	1.42(1)	1.36(2)	1.42(2)	1.40(4)	1.46(2)	1.36(4)
C–C (g)	1.505(6)	1.500(6)	1.52(1)	1.50(1)	1.55(3)	1.510(7)	1.52(2)

[a] D indicates the TMTTeN molecule. [b] Molecule A and molecule B represent two crystallographically independent molecules.

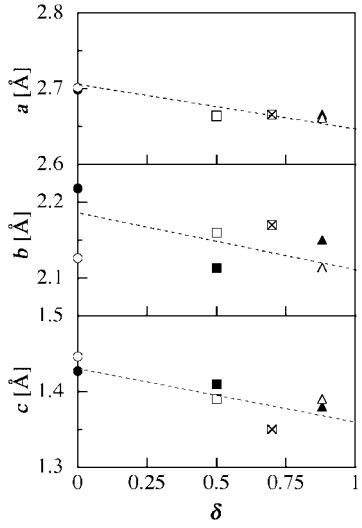

Figure 2. Formal charge (δ) dependences of three bond lengths of $TMTTeN^{+\delta}$ (*a*, *b* and *c*) that show large δ-dependence: neutral TMTTeN molecule A (open circles) and molecule B (black circles), $Ag(CN)_2^-$ salt (open squares), $Au(CN)_2^-$ salt (black squares), SCN^- salt (open triangles), ClO_4^- salt (black triangles), and AsF_6^- salt (x in box).

out as a result of the sum of the positive and negative Te···Te overlap integrals.

Crystal Structure Analyses

Neutral 2,3-DMTTeA Molecule

Figure 3 shows the crystal structure of the neutral 2,3-DMTTeA molecule recrystallized from carbon disulfide. There is one crystallographically independent donor molecule in the crystal. The 2,3-DMTTeA molecule has a planar structure. The molecular structure of 2,3-DMTTeA is subject to an orientational disorder that is caused by the unsymmetry of the molecule, which makes 2,3-DMTTeA appear as if it has a tetracene framework instead of the actual anthracene framework. Such an orientational disorder was not observed in the sulfur and selenium analogs of 2,3-DMTTeA.[15b] These facts indicate that the network formed by the tellurium atoms is very strong and dominant in terms of the construction of the crystal structures in comparison to the interaction between the anthracene moieties. As Figure 3 (parts a and b) indicate, the donor molecules form columns with a short interplanar distance of 3.78 Å along the *b*-axis, whereas a slip distance (5.41 Å) is very large along the donor short axis. Consequently, there is no intermolecular Te···Te contact that is less than the sum of the van der Waals radii (4.2 Å) in the donor columns. On the other hand, there are several short intercolumnar contacts, as shown in part b of Figure 3. To put it briefly, the molecules form side-by-side arrays along the *c*-axis through the short Te···Te contacts.

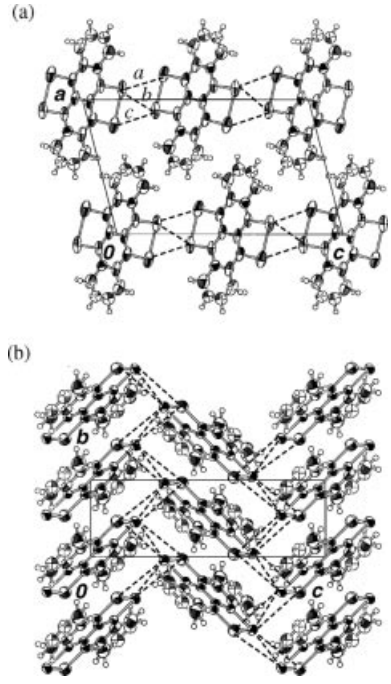

Figure 3. Crystal structures of the neutral 2,3-DMTTeA molecule projected on (a) the *ac*-plane and (b) the *bc*-plane. Owing to the orientational disorder, the occupation probability of two terminal CH_2 groups is 50%, and 2,3-DMTTeA molecule is drawn as if it has a tetracene framework. Intermolecular contacts [Å]: Te(1)···Te(2), a = 4.052(1); Te(1)···Te(2), b = 3.838(1); and Te(1)···Te(1), c = 4.100(1).

Neutral TMTTeN Molecule

An X-ray crystal structure analysis was performed on the neutral crystal of TMTTeN recrystallized from carbon disulfide. As shown in Figure 4 (part a and b), the crystal

includes carbon disulfide as an interstitial solvent. TMTTeN has no orientational disorder as in the molecular structure of 2,3-DMTTeA, because of the symmetrical shape of TMTTeN. Two kinds of crystallographically independent donor molecules (A and B) exist in the crystal (see Figure 4 (part a and b). Among them, molecule B is located on the inversion center. As Figure 4 (b) indicates, each of the donor molecules A and B form independent stacking columns along the *c*-axis. However, there is no intermolecular short Te···Te contact in both the donor columns of molecules A and B. On the other hand, there are several short intercolumnar intermolecular Te···Te contacts between the donor columns of molecules A and B, and the three-dimensional network formed by the protruded tellurium atoms of the donor molecules is developed in the crystal.

Cation Radical Salts of 2,3-DMTTeA

X-ray crystal structure analyses were performed on the cation radical salts of 2,3-DMTTeA with BF_4^-, ClO_4^-, ReO_4^-, PF_6^-, AsF_6^-, and Br^- anions. The BF_4^- and ReO_4^- salts are isostructural to the ClO_4^- salt and the PF_6^- salt is isostructural to the AsF_6^- salt. For this reason, only the crystal structures of the ClO_4^- and AsF_6^- salts are discussed among the tetrahedral and octahedral anion salts, respectively.

Crystal Structure of (2,3-DMTTeA)$_3$(ClO$_4$)$_2$

Overlap mode and crystal structure of the ClO_4^- salt of 2,3-DMTTeA are shown in Figure 5. The compositions of

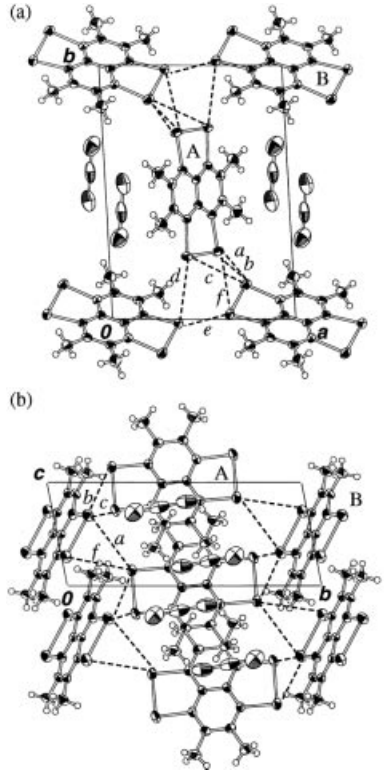

Figure 4. Crystal structures of the neutral TMTTeN molecule projected on (a) the *ab*-plane and (b) the *bc*-plane. Intermolecular contacts [Å]: Te(2)···Te(3), a = 4.0860(7); Te(2)···Te(3), b = 3.9032(8); Te(1)···Te(3), c = 3.820(1); Te(1)···Te(4), d = 3.9133(6); Te(4)···Te(4), e = 3.908(1); and Te(2)···Te(4), f = 3.8651(6).

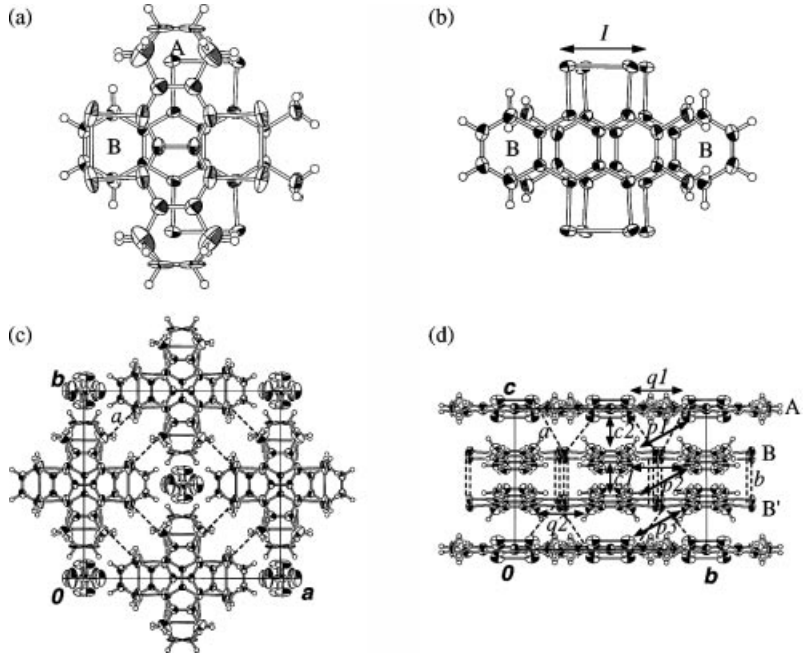

Figure 5. Overlap modes of the donor molecules in (2,3-DMTTeA)$_3$(ClO$_4$)$_2$ projected on the molecular planes (a) between molecules A and B, (b) between molecules B and B′. The occupation probability of two terminal CH_2 groups of molecule A is 50%. Interplanar distances [Å]: between molecules A and B, 3.81; and between molecules B and B′, 3.83. Slip distance [Å]: between molecules B and B′, I = 0.54. (c) Crystal structure of (2,3-DMTTeA)$_3$(ClO$_4$)$_2$ projected on the *ab*-plane. (d) Donor arrangement in (2,3-DMTTeA)$_3$(ClO$_4$)$_2$ viewed along the *a*-axis. Intermolecular contacts [Å]: Te(2)···Te(3), a = 4.1695(6); and Te(1)···Te(2), b = 3.9381(6). Overlap integrals ($\times 10^{-3}$): $c1$ = –24.75, $c2$ = 0.85, $p1$ = –0.96, $p2$ = 0.97, $p3$ = 0.53, $q1$ = 0.14, and $q2$ = 0.06.

the BF_4^-, ClO_4^-, and ReO_4^- salts were determined to be $(2,3\text{-DMTTeA})_3(\text{anion})_2$. There are two crystallographically independent fragments of the donor [a quarter (A) and a half (B) of the donor molecule] and a half of the ClO_4^- anion, resulting in an average oxidation state of the donor molecule of +2/3. The anion molecules are located in the channel surrounded by 2,3-DMTTeA molecules (see Figure 5, c). As shown in Figure 5 (a and b), molecule A has an orientational disorder of the anthracene moiety that is similar to the case of the neutral 2,3-DMTTeA molecule, whereas molecule B has no orientational disorder. Molecules A and B form A–B–B′-type stacking columns along the *c*-axis in which their long axes are rotated by 90° at the A–B overlap (see Figures 5, a and d). On the other hand, the overlap mode of molecules B and B′ is so-called "head-to-tail overlap" as shown in part b of Figure 5. As Figure 5 indicates (c and d), a three-dimensional Te···Te network is formed through several intermolecular short Te···Te contacts. The interplanar distance between molecules A and B (3.81 Å) is almost the same as that between molecules B and B′ (3.83 Å). On the contrary, the intracolumnar overlap integral between molecules A and B ($c2 = 0.85\times10^{-3}$) is much smaller than that between molecules B and B′ ($c1 = -24.75\times10^{-3}$) and is rather similar to those along the side-by-side directions ($p1 = -0.96\times10^{-3}$, $p2 = 0.97\times10^{-3}$, $p3 = 0.53\times10^{-3}$, $q1 = 0.14\times10^{-3}$, and $q2 = 0.06\times10^{-3}$), because the overlap mode between molecules A and B is not preferable and there is no short Te···Te contact between molecules A and B, where these intermolecular overlap integrals were calculated using the extended Hückel approximation. From the viewpoint of the intermolecular interaction, these results suggest the isolation of the dimers (molecules B and B′) in the donor column, giving rise to very low electrical conductivities of the tetrahedral anion salts ($\sigma_{rt} \approx 10^{-2}$ to 10^{-3} S cm^{-1}) as discussed later.

Crystal Structure of (2,3-DMTTeA)(AsF$_6$)$_{0.2}$

Figure 6 shows the overlap mode and crystal structure of the AsF_6^- salt of 2,3-DMTTeA. The orientational disorder of the 2,3-DMTTeA molecule is also observed in this salt. The compositions of the PF_6^- and AsF_6^- salts could not be determined by population refinement because of a heavy positional disorder of the anion molecules. Consequently, the compositions of $2,3\text{-DMTTeA}(\text{anion})_{0.2}$ were determined by electron probe microanalyses (EPMA). The anion molecules are located in the channels surrounded by the donor molecules, which is similar to the case of the tetrahedral anion salts. The anions are disordered along the donor stacking axis, and there are two kinds of possible positions of the AsF_6^- anion in a channel. Diffuse X-ray diffraction patterns are observed by an oscillation photograph and revealed that the AsF_6^- salt has a fivefold structure along the *a*-axis, suggesting that one AsF_6^- anion molecule exists per five unit cells. This result is consistent with the composition of the salt (5:1) determined by EPMA. As shown in Figure 6 (a and c), the donor molecules form uniform stacks along the *a*-axis. The dihedral angle of two donor molecules is 32.34° between the adjacent columns along the *b*-axis. An intermolecular interplanar distance is 3.81 Å and slip distances are 1.13 Å (*I*) and 1.21 Å (*II*) along the molecular long and short axes, respectively, indicating the relatively good overlap mode of the donors in the stack. As Figure 6 (b and c) indicates, there are several interstack Te···Te contacts [Te(1)···Te(1); a = 3.828(3) Å and Te(2)···Te(2); b = 3.882(3) Å] that are shorter than the intrastack one [Te(1)···Te(2); c = 4.155(2) Å]. The intermolecular interaction along the donor stacking direction shows a large overlap integral ($a1 = -20.96\times10^{-3}$) in comparison with the other ones ($c1 = -0.19\times10^{-3}$, $p1 = -2.22\times10^{-3}$, and $q1 = -0.46\times10^{-3}$). Hence, the intracolumnar conduction path of the AsF_6^- and PF_6^- salts is considered to be much better than those of the above-mentioned tetrahedral anion salts of 2,3-DMTTeA, but this salt showed a semiconducting behavior probably because of the strong one-dimensionality of the intermolecular interaction along the *a*-axis.

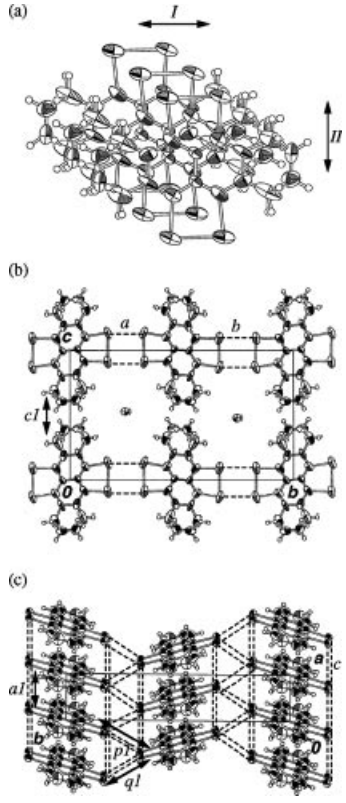

Figure 6. (a) Overlap mode of the donor molecules in $(2,3\text{-DMTTeA})(AsF_6)_{0.2}$ projected on the molecular planes. Interplanar distance [Å]: 3.81. Slip distances [Å]: I = 1.13 and II = 1.21. (b) Crystal structure of $(2,3\text{-DMTTeA})(AsF_6)_{0.2}$ projected on the *bc*-plane. (c) Donor arrangement in $(2,3\text{-DMTTeA})(AsF_6)_{0.2}$ viewed along the *c*-axis. Intermolecular contacts [Å]: Te(1)···Te(1), a = 3.828(3); Te(2)···Te(2), b = 3.882(3); and Te(1)···Te(1), c = 4.155(2). Overlap integrals ($\times10^{-3}$): $a1$ = –20.96, $c1$ = –0.19, $p1$ = –2.22, and $q1$ = –0.46. Dihedral angle between the adjacent donor molecules along the *b*-axis [°]: 32.34.

Crystal Structure of (2,3-DMTTeA)$_2$Br

The overlap mode and crystal structure of the Br^- salt of 2,3-DMTTeA are shown in Figure 7. In spite of use of the tetra-*n*-butylammonium salt of the $GaBr_4^-$ anion as a sup-

porting electrolyte, an EPMA measurement revealed that the gallium atom is not contained in the obtained crystal. The orientational disorder of the donor molecule is also observed in this salt. The composition was determined to be $(2,3\text{-DMTTeA})_2Br$ by EPMA. The anion molecules are disordered along the *c*-axis and occupy only one of two kinds of channels, which is surrounded by tellurium atoms of the donor molecule as if the anion avoids the steric hindrance of the outer benzene-ring of 2,3-DMTTeA molecules. As Figure 7 indicates, the donor arrangement of the Br^- salt is isostructural to that of a quasi one-dimensional metal $(TSeT)_2Cl$ with a tetragonal lattice, where TSeT is tetraselenotetracene, reported by Shibaeva et al. in 1978.[22,23] The donor molecules form uniform columns along the *c*-axis with a very short interplanar distance of 3.31 Å and a large slip distance along the molecular long axis (4.31 Å) (see Figure 7, a and c). The donor molecules are inclined with a dihedral angle of 53.99° between the adjacent donor columns. As shown in Figure 7 (b and c), no intermolecular Te···Te contact appears between the donor columns, whereas short contacts [Te(1)···Te(1); *a* = 3.699(4) Å] are developed in the column, suggesting a tight one-dimensional nature along the *c*-axis. The overlap integral between the donor molecules along the *c*-axis (*c1* = 53.81×10^{-3}) is very much larger than those of interstack ones (*p1* = -2.62×10^{-3}, *p2* = -1.22×10^{-3}, *q1* = -0.13×10^{-3}, and *q2* = -1.22×10^{-3}). These results also suggest its strong one-dimensional character along the stacking direction, which results in a quite high conductivity ($\sigma_{rt} \approx 1500\ S\,cm^{-1}$) and a semiconducting behavior.

Cation Radical Salts of TMTTeN

X-ray crystallographic analyses were performed on the cation radical salts of TMTTeN with $Ag(CN)_2^-$, $Au(CN)_2^-$, SCN^-, ClO_4^-, and AsF_6^- anions. Because the crystal structures of the $Ag(CN)_2^-$ and $Au(CN)_2^-$ salts are similar to each other, only the crystal structure of the $Ag(CN)_2^-$ salt is discussed here in respect of these two salts.

Crystal Structure of $(TMTTeN)_2Ag(CN)_2$

Figure 8 shows the overlap mode and crystal structure of the $Ag(CN)_2^-$ salt. The composition of the $Ag(CN)_2^-$ and $Au(CN)_2^-$ salts was determined to be $(TMTTeN)_2$(anion)

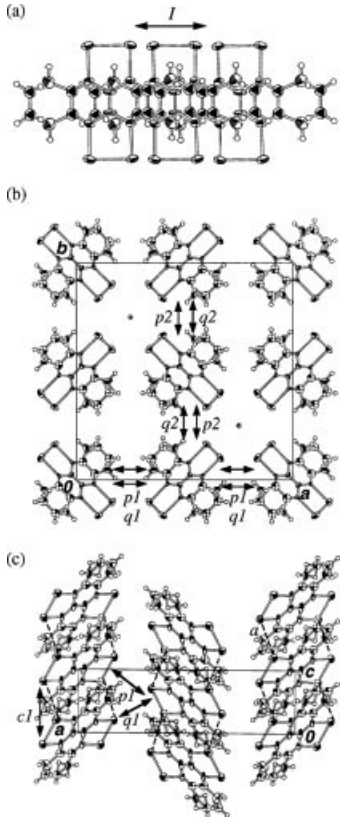

Figure 7. (a) Overlap mode of the donor molecules in $(2,3\text{-DMTTeA})_2Br$ projected on the molecular planes. Interplanar distance [Å]: 3.31. Slip distances [Å]: *I* = 4.31. (b) Tetragonal lattice of $(2,3\text{-DMTTeA})_2Br$ projected on the *ab*-plane. (c) Donor arrangement of $(2,3\text{-DMTTeA})_2Br$ viewed along the *b*-axis. Intermolecular contact [Å]: Te(1)···Te(1), *a* = 3.699(4). Overlap integrals ($\times10^{-3}$): *c1* = 53.81, *p1* = –2.62, *p2* = –1.22, *q1* = –0.13, and *q2* = –1.22. Dihedral angles between the adjacent donor molecules [°]: 53.99.

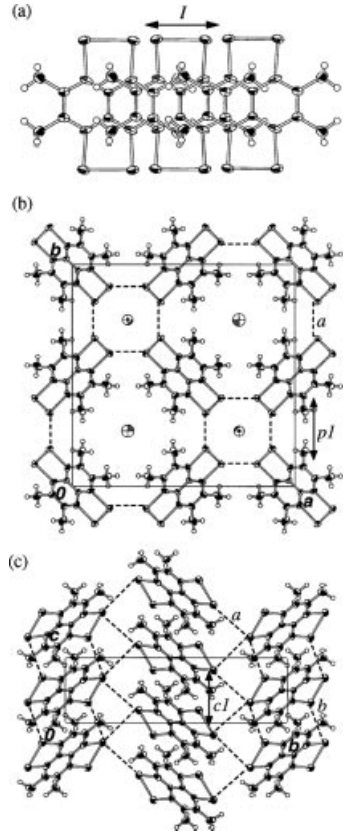

Figure 8. (a) Overlap mode of the donor molecules in $(TMTTeN)_2$-$Ag(CN)_2$. Interplanar distance [Å]: 3.41. Slip distance [Å]: *I* = 4.13. (b) Crystal structure of $(TMTTeN)_2Ag(CN)_2$ projected on the *ab*-plane. (c) Donor stacking columns of $(TMTTeN)_2Ag(CN)_2$ viewed along the *a*-axis. Intermolecular contacts [Å]: Te(1)···Te(1), *a* = 4.0199(8); and Te(1)···Te(1), *b* = 3.709(1). Overlap integrals ($\times10^{-3}$): *c1* = 90.96 and *p1* = –6.99. Dihedral angle between the adjacent donor molecules [°]: 71.4.

by a population refinement. The projections of the crystal structure of the $Ag(CN)_2^-$ salt on the *ab*- and *bc*-planes are shown in Figure 8 (b and c, respectively). The donor molecules are stacked along the *c*-axis and take the same orientation with a short interplanar distance of 3.41 Å and a large slip distance of 4.13 Å. The dihedral angle of the donor molecules is 71.4° between the adjacent donor columns. The $Ag(CN)_2^-$ anions are located on the 4_2-axes and are heavily disordered along the *c*-axis. However, the structure was refined to an R-factor of 3%. The crystal structure of this salt is quite similar to those of $(2,3\text{-DMTTeA})_2Br$ and $(TSeT)_2Cl$[23] with tetragonal lattices, but the positions of the anion molecules are different from the other salts. That is, the $Ag(CN)_2^-$ anions occupy all four channels in the unit cell that is surrounded by the donor molecule, because the methyl groups of TMTTeN are considerably smaller than the disordered large benzene ring of 2,3-DMTTeA and, as a result, there is enough space for the anions compared to $(2,3\text{-DMTTeA})_2Br$ (see Figure 8, b). As shown in Figure 8 (b and c), there are several intermolecular Te···Te contacts, and a three-dimensional network through tellurium atoms is developed between the intracolumns and intercolumns in contrast to the one-dimensional character of $(2,3\text{-DMTTeA})_2Br$. The one-dimensionality of the intermolecular interaction is weaker than that of $(2,3\text{-DMTTeA})_2Br$: $c1/p1 \approx 13$ in $(TMTTeN)_2Ag(CN)_2$, where $c1$ (90.96×10^{-3}) and $p1$ (-6.99×10^{-3}) are the overlap integrals parallel and perpendicular to the *c*-axis (the donor stacking axis), respectively, while $c1/p1 \approx 20$ in $(2,3\text{-DMTTeA})_2Br$, resulting in a stable metallic behavior of $(TMTTeN)_2Ag(CN)_2$ as discussed later.

Crystal Structure of (TMTTeN)(SCN)$_{0.88}$

The overlap mode and crystal structure of the SCN^- salt are shown in Figure 9. In spite of preparation from the solution containing both the SCN^- and ClO_4^- anions, the composition of the obtained salt was determined to be $(TMTTeN)(SCN)_{0.88}$ by a population refinement and no ClO_4^- anion was discovered, which is consistent with the result of the EPMA measurement that shows no trace of chlorine atom. Although the crystals of the SCN^- salt with the same shape were also prepared from the solution that contains only the SCN^- anion by an electrocrystallization, the obtained crystals were very small. The projections of the crystal structure of the SCN^- salt on the *bc*-, *ab*- and *ac*-planes are shown in parts b–d in Figure 9. The donor molecules are stacked to form columns along the *a*-axis with a short intermolecular interplanar distance of 3.62 Å and a large slip distance of 4.03 Å. The anions are located in the channels that are formed by TMTTeN molecules. The donor molecules are inclined with a dihedral angle of 72.2° between the two adjacent donor columns along the *b*-axis. The donor arrangement of $(TMTTeN)(SCN)_{0.88}$ is almost

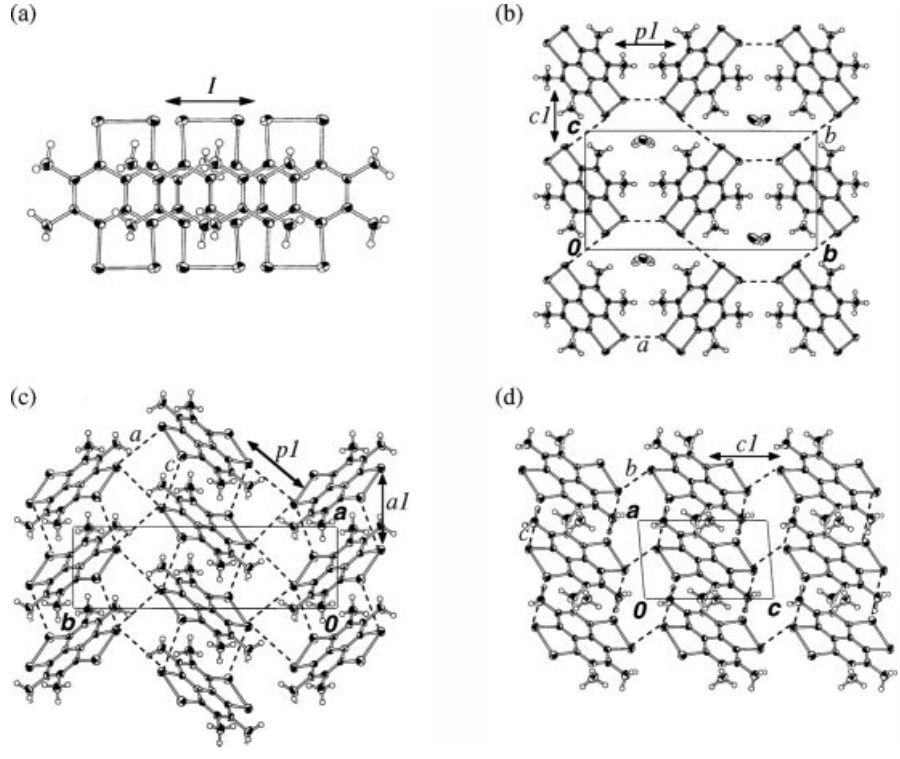

Figure 9. (a) Overlap mode of donor molecules in $(TMTTeN)(SCN)_{0.88}$. Interplanar distance [Å]: 3.62. Slip distance [Å]: I = 4.03. (b) Crystal structure of $(TMTTeN)(SCN)_{0.88}$ projected on the *bc*-plane. Donor stacking columns of $(TMTTeN)(SCN)_{0.88}$ viewed (c) along the *c*-axis and (d) along the *b*-axis. Intermolecular contacts [Å]: Te(1)···Te(1), a = 4.048(1); Te(2)···Te(2), b = 4.123(1); and Te(1)···Te(2), c = 3.788(2). Overlap integrals ($\times10^{-3}$): $a1$ = 82.83, $c1$ = –24.36, and $p1$ = –7.23. Dihedral angle between the adjacent donor molecules along the *b*-axis [°]: 72.2.

the same as that of previously reported $(TSeT)_2SCN$.[23,24] This crystal structure belongs to a monoclinic lattice and is not isostructural to those of the $Ag(CN)_2^-$ and $Au(CN)_2^-$ salts with tetragonal lattices. That is, the penetration of the SCN^- anion into the TMTTeN lattice results in a modification of the packing pattern of TMTTeN molecules along the *c*-axis of the crystals, but the arrangements of TMTTeN molecules along the other two axes are almost the same as those of the $Ag(CN)_2^-$ and $Au(CN)_2^-$ salts. On the other hand, the atomic positions of the SCN^- anions are disordered along the donor stacking axis. As shown in Figure 9 (b–d), there are many intermolecular Te···Te contacts and a three-dimensional network is developed through tellurium atoms in the crystal. The overlap integral along the stack is fairly large ($a1 = 82.83 \times 10^{-3}$) compared to the others ($c1 = -24.36 \times 10^{-3}$ and $p1 = -7.23 \times 10^{-3}$) because of the tight stacking structure of TMTTeN molecules. On the other hand, the interstack overlap integral *c1* is about three times larger than *p1* because of a parallel arrangement of two TMTTeN molecules in the interaction *c1* in contrast to an almost orthogonal arrangement in the interaction *p1*. The large interaction *c1* also originates from the structural situation where two intermolecular Te···Te overlaps between each tellurium pair with longer Te···Te distance and shorter Te···Te distance cannot cancel each other out in spite of the nodal plane at the Te–Te bond. Thus, the overlap integral along the stacking axis (*a1*) is only three times larger than that of the side-by-side direction (*c1*), suggesting relatively strong quasi two-dimensionality in the *ac*-plane, which results in a stable metallic behavior down to 4.2 K.

Crystal Structure of (TMTTeN)$(ClO_4)_{0.88}$

The overlap mode and crystal structure of the ClO_4^- salt are shown in Figure 10. The composition of the ClO_4^- salt was determined to be $(TMTTeN)(ClO_4)_{0.88}$ by a population refinement. The donor arrangement of the ClO_4^- salt is a little different from those of the $Ag(CN)_2^-$ and $Au(CN)_2^-$ salts. Namely, the donor molecules form the columns with uniform stackings along the *c*-axis and the anion molecules are disordered along the donor stacking axis on the special position of the 4_2-axes in a similar manner to the $Ag(CN)_2^-$ and $Au(CN)_2^-$ salts. However, the gradient between the donor molecules is very gentle, with a dihedral angle of 26.9° between the two adjacent donor columns, compared to that of the $Ag(CN)_2^-$ salt (71.4°). As it turned out, the lattice constants of the *a*- and *b*-axes of the ClO_4^- salts are longer by about 2.4 Å, and the *c*-axis of the ClO_4^- salt is shorter by about 1.3 Å than those of the $Ag(CN)_2^-$ and $Au(CN)_2^-$ salts. Furthermore, the donor molecule has a small slip distance (1.08 Å), but the interplanar distance (3.87 Å) is larger than that of the $Ag(CN)_2^-$ salt (3.41 Å) (see parts a in Figure 8 and Figure 10). This large interplanar distance might be related to a larger positive charge on the TMTTeN molecule (+0.88) than the case of the $Ag(CN)_2^-$ salt (+0.5). As shown in Figure 10 (b and c), a three-dimensional network mediated by tellurium atoms that is similar to the other TMTTeN salts is developed in the crystal. Consequently, not only a strong intermolecular interaction is observed in the donor stacking direction (*c1* $= -80.61 \times 10^{-3}$), but a comparatively strong interaction also exists between stacking columns ($p1 = -5.45 \times 10^{-3}$). However, this salt showed a semiconducting behavior with a relatively low conductivity of $\sigma_{rt} \approx 0.8\ S\,cm^{-1}$, probably because of the difference of the stacking mode of the donors.

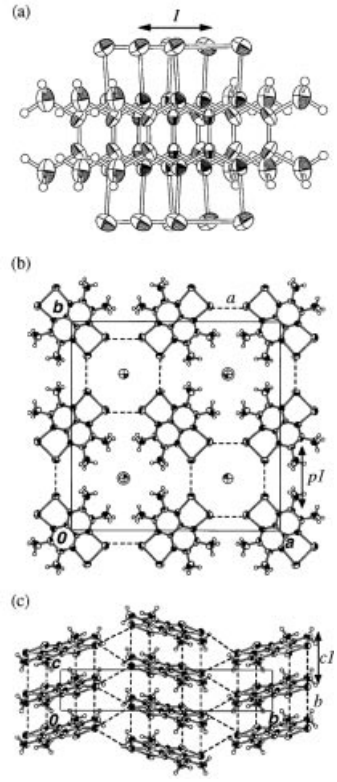

Figure 10. (a) Overlap mode of the donor molecules in (TMTTeN)$(ClO_4)_{0.88}$. Interplanar distance [Å]: 3.87. Slip distance [Å]: $I = 1.08$. (b) Crystal structure of $(TMTTeN)(ClO_4)_{0.88}$ projected on the *ab*-plane. (c) Donor stacking columns of $(TMTTeN)(ClO_4)_{0.88}$ viewed along the *a*-axis. Intermolecular contacts [Å]: Te(1)···Te(1), $a = 4.112(2)$; and Te(1)···Te(1), $b = 4.020(2)$. Overlap integrals ($\times 10^{-3}$): $c1 = -80.61$ and $p1 = -5.45$. Dihedral angle between the adjacent donor molecules [°]: 26.9.

Crystal Structure of (TMTTeN)$(AsF_6)_{0.7}$

Figure 11 shows the overlap mode and crystal structure of the AsF_6^- salt. The space group of this salt ($P42_1m$) is different from the other tetragonal salts ($P4_2/ncm$), and a half of the donor molecule is a crystallographically independent unit. The composition of the AsF_6^- salts is determined to be $(TMTTeN)(AsF_6)_{0.7}$ by a population refinement. The donor arrangement, interplanar distance of 3.44 Å and slip distance of 4.06 Å in the AsF_6^- salt is almost the same as those of the $Ag(CN)_2^-$ salt, suggesting that the donor molecules of these salts possess almost the same degree of positive charge. Although the anion molecules are located on all four channels that are formed by the donor molecules, only the anions in the two channels that are surrounded by tellurium atoms of the donor molecules are disordered along the *c*-axis. As shown in Figure 11 (b and c), a three-dimensional network through tellurium atoms is also devel-

oped and is similar to the linear anion salts like the $Ag(CN)_2^-$ and $Au(CN)_2^-$ salts. Intermolecular overlap integrals are comparatively large ($c1 = 89.01\times10^{-3}$, $p1 = -8.60\times10^{-3}$, $p2 = -8.63\times10^{-3}$, $q1 = -7.08\times10^{-3}$, and $q2 = -6.80\times10^{-3}$).

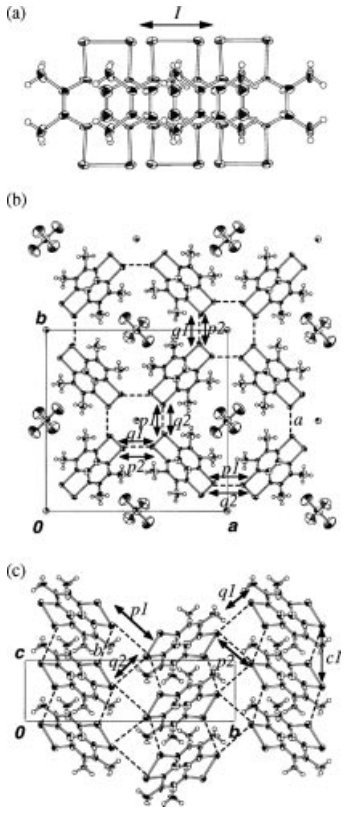

Figure 11. (a) Overlap mode of the donor molecules in $(TMTTeN)(AsF_6)_{0.7}$. Interplanar distance [Å]: 3.44. Slip distance [Å]: $I = 4.06$. (b) The crystal structure of $(TMTTeN)(AsF_6)_{0.7}$ projected on the *ab*-plane. (c) Donor stacking columns of $(TMTTeN)(AsF_6)_{0.7}$ along the *a*-axis. Intermolecular contacts [Å]: Te(1)···Te(2), $a = 4.054(3)$; and Te(1)···Te(2), $b = 3.716(2)$. Overlap integrals ($\times10^{-3}$): $c1 = 89.01$, $p1 = -8.60$, $p2 = -8.63$, $q1 = -7.08$ and $q2 = -6.80$. Dihedral angle between the adjacent donor molecules [°]: 65.24.

Physical Properties

Conducting Properties of the 2,3-DMTTeA Salts

Room temperature conductivities and activation energies of the obtained 2,3-DMTTeA salts are summarized in Table 2. The resistivities of the BF_4^-, ClO_4^-, ReO_4^-, PF_6^-, AsF_6^-, and SbF_6^- salts were measured down to about 80 K along the donor stacking axes. The BF_4^-, ClO_4^-, and ReO_4^- salts showed semiconducting behaviors with low conductivities of $\sigma_{rt} \approx 10^{-2}$ to 10^{-3} S cm^{-1} owing to their inadequate conduction paths along the donor stacking axes that originate from the crossed overlap mode of molecules A and B (Figure 5) and the strong dimerization of molecules B and B′. The temperature dependence of electrical resistivities of the PF_6^-, AsF_6^-, and SbF_6^- salts are also semiconducting with relatively high room temperature conductivities of 1.0–20 S cm^{-1} and low activation energies of 0.02–0.09 eV because of their quasi one-dimensional structures that indicate a strong one-dimensional nature along the donor stacking axis. On the other hand, the Br^- and SCN^- salts showed quite high conductivities of σ_{rt} = 1300 and 890 S cm^{-1} and semiconducting behaviors with very low activation energies of 0.01 and 0.004 eV, respectively, owing to the tight one-dimensional character along the donor stacking direction and the disorders of the donor and anion molecules. The CuI_2^- salt showed a semiconducting behavior with a low room temperature conductivity of 10^{-3} S cm^{-1} and a large activation energy of 0.17 eV. The NO_3^- salt indicates a semiconducting behavior with a relatively large room temperature conductivity of 4.7 S cm^{-1} and a large activation energy of 0.031 eV. As a result, no metallic salt has been discovered in the 2,3-DMTTeA salts, probably because of the strong one-dimensionality of their electronic structures and the disorder effect of 2,3-DMTTeA molecules in the crystal.

Conducting Properties of the TMTTeN Salts

Room temperature conductivities and activation energies of the TMTTeN salts are listed in Table 3. All the salts except for the $Ag(CN)_2^-$, $Au(CN)_2^-$, and SCN^- salts are semiconductors or insulators. Among them, the $Cu(SCN)_2^-$ and

Table 2. Electrical properties of the 2,3-DMTTeA salts.[a]

Anions[b]	Solvents[c]	Current [μA]	Electrical properties	$\sigma_{293\,K}$ [S cm^{-1}]	E_a [eV]
BF4$^-$	THF	0.05–0.3	semiconducting	9.7×10^{-3}	0.17
ClO4$^-$	THF or PhCl	0.05–0.2	semiconducting	7.1×10^{-3}	0.16
ReO_4^-	THF	0.1–0.7	semiconducting	5.5×10^{-3}	0.16
PF_6^-	THF	0.1–0.3	semiconducting	1.0	0.090
AsF_6^-	THF	0.1–0.5	semiconducting	17	0.019
SbF_6^-	THF	0.1–0.5	semiconducting	10	0.048
Br^-[d]	THF	0.1–0.7	semiconducting	1300	0.010
SCN^-	TCE	0.1–0.4	semiconducting	890	0.004
CuI_2^-	THF	0.1–0.3	semiconducting	3.0×10^{-3}	0.17
NO_3^-	THF	0.05–0.3	semiconducting	4.7	0.031

[a] All preparations were carried out at room temperature under nitrogen. [b] All the supporting electrolytes were tetra-*n*-butylammonium salts except for the $GaBr_4^-$ anion. Tetraethylammonium salt was used in the $GaBr_4^-$ salt. [c] THF = tetrahydrofuran, PhCl = chlorobenzene and TCE = 1,1,2-trichloroethane. [d] This salt was prepared with tetra-*n*-butylammonium salt of $GaBr_4^-$ as a supporting electrolyte.

Table 3. Electrical properties of the TMTTeN salts.[a]

Anions[b]	Solvents[c]	Current [μA]	Electrical properties	$\sigma_{293\,K}$ [S cm^{-1}]	E_a [eV]
$Ag(CN)_2^-$	10% EtOH/TCE	0.1–0.2	metallic down to ca. 50 K	760	
$Au(CN)_2^-$	10% EtOH/TCE	0.1–0.2	metallic down to ca. 50 K	720	
SCN^-[d]	10% EtOH/TCE	0.1–0.2	metallic down to 4.2 K	590	
$Cu(SCN)_2^-$	THF	0.1	semiconducting	840	0.055
$N(CN)_2^-$	PhCN	0.1	insulating	$<10^{-6}$	
BF_4^-	10% EtOH/PhCl	0.1	semiconducting	9.9	0.11
ClO_4^-	PhCl	0.1	semiconducting	7.6×10^{-1}	0.072
$GaBr_4^-$	10% EtOH/PhCl	0.1	semiconducting	360	0.028
PF_6^-	10% EtOH/PhCl	0.1	semiconducting	7.7×10^{-1}	0.054
AsF_6^-	10% EtOH/PhCl	0.1	semiconducting	13	0.015
SbF_6^-	THF or PhCl	0.1	semiconducting	3.0×10^{-1}	0.10
Br^-	10% EtOH/PhCl	0.1	semiconducting	6.0×10^{-2}	0.12
$Mo_6O_{19}^{2-}$	10% EtOH/PhCl	0.1	semiconducting	2.4	0.038

[a] All preparations were carried out at 40 °C under nitrogen. [b] All the supporting electrolytes were tetra-*n*-butylammonium salts except for the $Cu(SCN)_2^-$, $N(CN)_2^-$, BF_4^-, and SbF_6^- salts. Tetraethylammonium salt was used in the BF_4^- salt and tetraphenylphosphonium salt was used in the $N(CN)_2^-$ salt. In the $Cu(SCN)_2^-$ and SbF_6^- salts, bis(triphenylphosphoranylidene)ammonium salts were used. [c] EtOH = ethanol, TCE = 1,1,2-trichloroethane, THF = tetrahydrofuran, PhCN = benzonitrile and PhCl = chlorobenzene. [d] This salt was prepared under existence of two kinds of anion complexes, tetra-*n*-butylammonium salts of SCN^- and ClO_4^- anions.

$GaBr_4^-$ salts showed very high room temperature conductivities of 840 and 360 S cm^{-1} with low activation energies of 0.02–0.04 eV, respectively. On the other hand, the ClO_4^- salt showed a low room temperature conductivity of 10^{-1} S cm^{-1}. The linear $Ag(CN)_2^-$, $Au(CN)_2^-$, and SCN^- anion salts showed very high room temperature conductivities (590–760 S cm^{-1}). As shown in Figure 12, the temperature dependences of the resistivities of the $Ag(CN)_2^-$ and $Ag(CN)_2^-$ salts are metallic down to about 50 K, below which the resistivities increase very slowly down to 4.2 K with decreasing temperature. On the other hand, Figure 12 also shows that the temperature dependence of electrical resistivities of the SCN^- salt is metallic down to 4.2 K without any increase of resistivities, in contrast to the $Ag(CN)_2^-$ and $Ag(CN)_2^-$ salts. Although the temperature dependence of its resistivity is very small, like those of the $Ag(CN)_2^-$ and $Au(CN)_2^-$ salts, this SCN^- salt displays no increase in resistivity. Therefore, the SCN^- salt is revealed to be a genuine stable metal down to low temperatures. As mentioned before, this system has a strong transverse intermolecular interaction (see *c1* in Figure 9), which is the origin of its stable metallic state. On the other hand, the AsF_6^- salt also has a relatively high conductivity of 13 S cm^{-1}, but showed a semiconducting behavior at room temperature. Considering it has almost the same donor arrangement as the metallic $Ag(CN)_2^-$ and $Au(CN)_2^-$ salts, this semiconducting behavior may suggest that the large disorder effect of the octahedral AsF_6^- anion prevents a metallic conducting behavior.

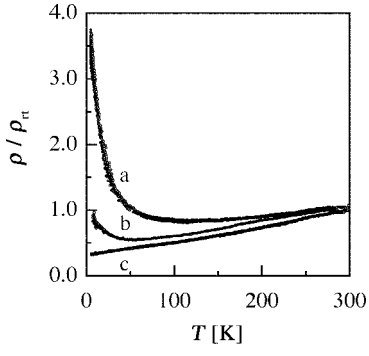

Figure 12. Temperature dependence of the electrical resistivities of the metallic TMTTeN salts. a, $(TMTTeN)_2Au(CN)_2$; b, $(TMTTeN)_2Ag(CN)_2$; and c, $(TMTTeN)(SCN)_{0.88}$.

Magnetic Properties of the TMTTeN Salts

The magnetic susceptibilities of $(TMTTeN)_2Ag(CN)_2$ and $(TMTTeN)(SCN)_{0.88}$ were measured using SQUID magnetometer down to 2 K at 30 kOe. The susceptibility of the neutral TMTTeN crystal was also measured in order to estimate the diamagnetic contribution of the TMTTeN molecule, which was performed by subtracting that of carbon disulfide included in the crystal of the neutral TMTTeN molecule. Figure 13 shows the temperature dependence of paramagnetic susceptibilities of $(TMTTeN)_2Ag(CN)_2$ and $(TMTTeN)(SCN)_{0.88}$. The paramagnetic susceptibility of $(TMTTeN)_2Ag(CN)_2$, which is corrected by subtracting a diamagnetic contribution and a small low-temperature Curie component due to paramagnetic impurities and/or lattice defects, was almost constant throughout the temperature range, indicating a Pauli paramagnetism based on metal electrons ($2.0–2.5\times10^{-4}$ emu mol^{-1}). No anomaly that corresponds to the gradual resistivity increase around 50 K was observed, suggesting the stable metallic nature of this salt. On the other hand, the paramagnetic susceptibilities of $(TMTTeN)(SCN)_{0.88}$ are also almost constant throughout the temperature range, indicating the Pauli paramagnetism of the system ($1.6–1.9\times10^{-4}$ emu mol^{-1}). Therefore, as revealed by the low-temperature resistivity behaviors, these salts are the first systems that possess metallic ground state among the *peri*-ditellurium-bridged donors. Because these TMTTeN conductors have an approximately one-dimensional cosine band along the molecular stacking direction, the smaller susceptibility of $(TMTTeN)(SCN)_{0.88}$ and larger susceptibility of $(TMTTeN)_2Ag(CN)_2$ seem to be related to the difference in not only their bandwidths but also their band-

fillings; namely, the ratio $\sin(\pi \times 0.5/2)/\sin(\pi \times 0.88/2) \approx 0.72$, is nearly equal to the ratio of the susceptibilities of these salts. In addition, the magnitude of these susceptibilities is about half that of the well-known κ-type BEDT-TTF superconductors ($\approx 5 \times 10^{-4}$ emu mol^{-1}),[25] where BEDT-TTF is bis(ethylenedithio)-TTF. Their small susceptibilities suggest large bandwidths of $(TMTTeN)_2Ag(CN)_2$ and $(TMTTeN)(SCN)_{0.88}$, which are brought about by the strong intermolecular interaction, and are consistent with the organic metals based on tellurium-containing donors such as (TTeF)(TCNQ).[26]

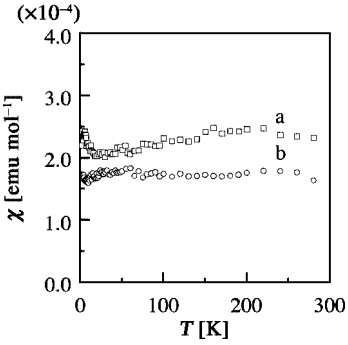

Figure 13. Temperature dependence of the paramagnetic susceptibilities of the TMTTeN salts. a, $(TMTTeN)_2Ag(CN)_2$; and b, $(TMTTeN)(SCN)_{0.88}$.

Band Structure Calculations

We have previously reported the results of the extended Hückel tight-binding band calculation on $(TMTTeN)_2Ag(CN)_2$.[18] However, the extended Hückel tight-binding band is calculated anew, because the empirical parameters used here are redetermined on the basis of the results of the ab initio MO calculations. As the first step of the band structure calculation, an extended Hückel MO was obtained as approximately the same as the ab initio MO. The calculated intermolecular overlap integrals of the individual salts have already been presented, together with their crystal structures. Generally speaking, the transverse interactions became much smaller than the interaction along the direction of the molecular stacking, because of the nodal plane at the Te–Te bond. The energy dispersion curves of conduction bands and the Fermi surfaces of $(TMTTeN)_2Ag(CN)_2$ and $(TMTTeN)(SCN)_{0.88}$ are shown in Figures 14 and 15, respectively.

Energy Dispersion Curves and Fermi Surface of $(TMTTeN)_2Ag(CN)_2$

Owing to the tetragonal lattice symmetry, the obtained band dispersions are doubly degenerated on the XM line (see Figure 14), which makes the Fermi surfaces that are composed of two corrugated one-dimensional Fermi surfaces quasi three-dimensional. A large bandwidth (≈4.0 eV) is consistent with the observed small Pauli susceptibility. The Fermi surfaces are closed in the a^*c^*- and b^*c^*-planes and also in the plane perpendicular to the c^*-axis [an example of the cross section of the Fermi surface at the plane (Γ′X′Y′) perpendicular to the c^*-axis is presented], as shown in Figure 14. As mentioned before, the analogous selenium-donor system $(TSeT)_2Cl$ showed a metal–semi-

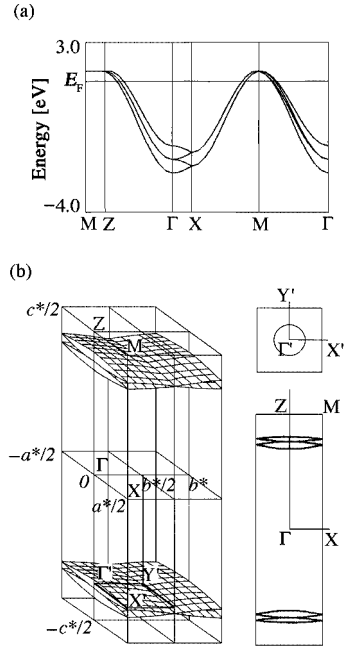

Figure 14. Energy band structures and three-dimensional Fermi surfaces of $(TMTTeN)_2Ag(CN)_2$ obtained by the extended Hückel tight-binding band calculation and their cross sections at the plane through ΓXZ and Γ′X′Z′, where Γ = (0, 0, 0), X = (a^*/2, 0, 0), Z = (0, 0, c^*/2), Γ′ = (0, 0, –0.35c^*), X′ = (a^*/2, 0, –0.35c^*), and Y′ = (0, b^*/2, –0.35c^*).

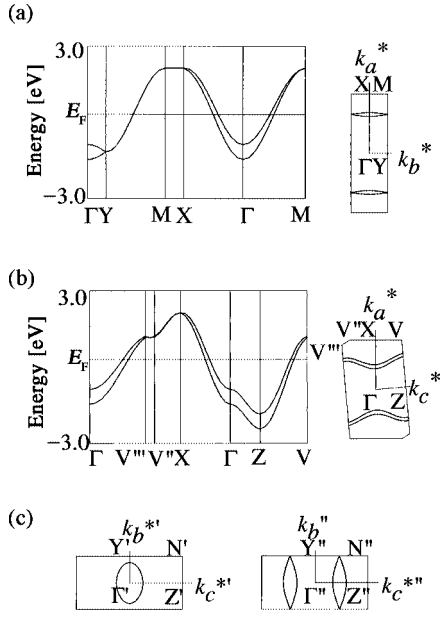

Figure 15. Energy band structures and cross sections of Fermi surfaces of $(TMTTeN)(SCN)_{0.88}$ obtained by the extended Hückel tight-binding band calculation. Γ = (0, 0, 0), X = (a^*/2, 0, 0), Y = (0, b^*/2, 0), Z = (0, 0, c^*/2), Γ′ = (0.23a^*, 0, 0), Y′ = (0.23a^*, b^*/2, 0), Z′ = (0.23a^*, 0, c^*/2), Γ″ = (0.28a^*, 0, 0), Y″ = (0.28a^*, b^*/2, 0), and Z″ = (0.28a^*, 0, c^*/2).

metal transition around 20 K, where a susceptibility drop that indicates a partial disappearance of the Fermi surfaces was observed. The stable metallic state of $(TMTTeN)_2Ag(CN)_2$ is attributable to the stronger three-dimensionality of the band structure. Therefore, $(TMTTeN)_2Ag(CN)_2$ is the first organic conductor that has a stable metallic state and "quasi three-dimensional Fermi surfaces" at ambient pressure on the basis of the tellurium-containing π donors.

Energy Dispersion Curves and Fermi Surface of (TMTTeN)(SCN)$_{0.88}$

As Figure 15a indicates, the band dispersions are doubly degenerated on the YM line. A large bandwidth (≈4.5 eV) is consistent with the observed small Pauli susceptibility. The Fermi surface of the SCN^- salt is open along the *b**- and *c**-directions, but the intermolecular interactions between the donor columns are fairly strong, as mentioned before. As shown in part c of Figure 15, cross sections of the Fermi surface perpendicular to the *a**-axis indicate a two- or quasi two-dimensional metallic state. Consequently, the Fermi surfaces are considered to be stable against the nesting of the Fermi surfaces. This may be an origin of the stable metallic state of the SCN^- salt.

Conclusions

Crystal structures and physical properties of various cation radical salts based on the *peri*-ditellurium-bridged polyacene donor molecules 2,3-DMTTeA and TMTTeN were examined. We have obtained the stable metallic cation radical salts of the TMTTeN molecule. Compared with usual organic conductors, the molecular conductors based on these tellurium-containing π donors show a very strong tendency to form a three-dimensional network mediated by tellurium atoms. Owing to the strong Te···Te network, the anions have very small contributions to the architecture of the crystal structures and are located fairly randomly in the channels that are formed by the donor molecules in most cases. New conducting systems with ordered crystal structures will be obtained by suitable selection of counteranions, which will afford a new class of three-dimensional organic metals with bandwidths much wider than the hitherto-obtained organic metals.

Experimental Section

General Remarks: 2,3-DMTTeA and TMTTeN were synthesized according to the reported methods.[15,16] Tetrahydrofuran (THF) was freshly distilled from sodium and benzophenone under nitrogen prior to use. Chlorobenzene (PhCl) was washed three times with concd. sulfuric acid, then with aqueous sodium hydrogen carbonate solution and water, followed by drying with calcium chloride and distilled from diphosphorus pentaoxide. Ethanol (EtOH) was distilled from magnesium ethoxide under nitrogen. Benzonitrile (PhCN) was dried with calcium chloride and distilled from diphosphorus pentaoxide under reduced pressure. 1,1,2-Trichloroethane (TCE) was washed three times with concd. sulfuric acid, then with aqueous sodium hydrogen carbonate solution and water, followed by drying with calcium chloride and was distilled under nitrogen. All the supporting electrolytes were recrystallized several times with organic solvents.

Electrocrystallization: The crystals of cation radical salts were grown by an electrochemical oxidation in the solvent shown in Table 2 for the 2,3-DMTTeA salts and Table 3 for the TMTTeN salts in the presence of the donor and the tetraalkylammonium, tetraphenylphosphonium, or bis(triphenylphosphoranylidene)ammonium salts of the corresponding anions under a constant current of 0.05–0.7 μA at room temperature in the case of the 2,3-DMTTeA salts and at 40 °C in the case of the TMTTeN salts.

Crystal Structure Determination: X-ray crystal structure analyses were performed on the neutral 2,3-DMTTeA and TMTTeN molecules recrystallized from carbon disulfide and their cation radical salts. Intensity data were measured with Rigaku AFC5R or AFC7R automated four-circle diffractometers or R-AXIS IV imaging plate area detector [only for $TMTTeN(AsF_6)_{0.7}$] by using graphite-monochromated Mo-K_α radiation at room temperature. Experimental details and crystal data are listed in Table 4, Table 5, and Table 6. Anisotropic temperature factors were applied for the non-hydrogen atoms. The calculated positions of hydrogen atoms were not refined but included in the final calculation. All calculations were performed using the teXsan[27] crystallographic software package of the Molecular Structure Corporation. CCDC-118377–118378, 121877–121880, 142670, and 264456–264461 contain the supplementary crystallographic data for this paper. These data can be obtained free of charge from The Cambridge Crystallographic Data Centre via www.ccdc.cam.ac.uk/data_request/cif.

Table 4. Crystallographic data of the neutral 2,3-DMTTeA and TMTTeN.

	2,3-DMTTeA	TMTTeN·CS_2
Formula	$C_8H_5Te_2$	$C_{15}H_{12}S_2Te_4$
Formula mass	356.33	766.78
Crystal color, habit	black, needle	black, rod
Crystal system	monoclinic	triclinic
a [Å]	9.976(5)	10.812(5)
b [Å]	5.137(1)	14.588(6)
c [Å]	16.186(1)	6.295(3)
α [°]		100.49(4)
β [°]	104.28(2)	106.75(4)
γ [°]		89.90(4)
V [Å^3]	803.8(3)	933.5(7)
Space group	$P2_1/c$ (#14)	$P\bar{1}$ (#2)
Z	4	2
$D_{calcd.}$ [g cm^{-3}]	2.944	2.728
μ(Mo-K_α) [cm^{-1}]	71.75	64.04
Diffractometer	Rigaku AFC7R	Rigaku AFC5R
Radiation	Mo-K_α (λ = 0.71069 Å)	Mo-K_α (λ = 0.71069 Å)
Temperature [K]	294	296
Measured reflections	total: 2722, unique: 2588	total: 5714, unique: 5445
Structure solution	Direct methods (SHELXS86)	Direct methods (SHELXS86)
Refinement	Full-matrix least-squares	Full-matrix least-squares
No. observations	1200 [$I>3.00\sigma(I)$]	3883 [$I>3.00\sigma(I)$]
No. variables	90	190
Residuals: R;[a] R_w[b]	0.054; 0.040	0.034; 0.033

[a] $R = \Sigma||F_o| - |F_c||/\Sigma|F_c|$. [b] $R_w = [\Sigma\omega(|F_o| - |F_c|)^2/\Sigma\omega F_o^2]^{1/2}$.

Electron Probe Microanalysis (EPMA): Several single crystals were attached on a carbon tape, and several points on each crystal were examined by Scanning Electron Microscope, S-450 (Hitachi, Co.

Table 5. Crystallographic data of the 2,3-DMTTeA salts.

	(2,3-DMTTeA)$_3$(BF$_4$)$_2$	(2,3-DMTTeA)$_3$(ClO$_4$)$_2$
Formula	$C_{12}H_{7.50}B_{0.50}F_2Te_3$	$C_{12}H_{7.50}Cl_{0.50}O_2Te_3$
Formula mass	577.89	584.22
Crystal color, habit	black, prismatic	black, prismatic
Crystal system	monoclinic	monoclinic
a [Å]	16.437(5)	16.538(3)
b [Å]	14.585(4)	14.681(2)
c [Å]	11.623(4)	11.612(4)
β [°]	111.19(2)	111.48(2)
V [Å^3]	2597(1)	2623(1)
Space group	$C2/m$ (#12)	$C2/m$ (#12)
Z	8	8
$D_{calcd.}$ [g cm^{-3}]	2.955	2.958
μ(Mo-K_α) [cm^{-1}]	66.92	67.17
Diffractometer	Rigaku AFC7R	Rigaku AFC7R
Radiation	Mo-K_α (λ = 0.71069 Å)	Mo-K_α (λ = 0.71069 Å)
Temperature [K]	295	295
Measured reflections	total: 4067, unique: 3941	total: 4146, unique: 3974
Structure solution	Direct methods (SHELX86)	Direct methods (SIR92)
Refinement	full-matrix least-squares	full-matrix least-squares
No. observations	2614 [I>3.00$\sigma(I)$]	2568 [I>3.00$\sigma(I)$]
No. variables	164	169
Residuals: R;[a] R_w[b]	0.052; 0.049	0.034; 0.023
	(2,3-DMTTeA)$_3$(ReO$_4$)$_2$	(2,3-DMTTeA)$_5$PF$_6$
Formula	$C_{12}H_{7.50}O_2Re_{0.50}Te_3$	$C_8H_5F_{0.60}P_{0.10}Te_2$
Formula mass	659.59	370.82
Crystal color, habit	black, prismatic	black, prismatic
Crystal system	monoclinic	monoclinic
a [Å]	16.617(2)	4.155(2)
b [Å]	14.990(2)	19.854(8)
c [Å]	11.569(2)	11.519(4)
β [°]	111.015(9)	94.66(4)
V [Å^3]	2690.0(6)	947.0(6)
Space group	$C2/m$ (#12)	$P2_1/a$ (#14)
Z	8	4
$D_{calcd.}$ [g cm^{-3}]	3.257	2.601
μ(Mo-K_α) [cm^{-1}]	109.29	61.20
Diffractometer	Rigaku AFC5R	Rigaku AFC7R
Radiation	Mo-K_α (λ = 0.71069 Å)	Mo-K_α (λ = 0.71069 Å)
Temperature [K]	296	296
Measured reflections	total: 4196, unique: 4069	total: 2548, unique: 2256
Structure solution	Direct methods (SIR92)	Direct methods (SIR92)
Refinement	Full-matrix least-squares	Full-matrix least-squares
No. observations	2281 [I>3.00$\sigma(I)$]	1182 [I>3.00$\sigma(I)$]
No. variables	172	109
Residuals: R;[a] R_w[b]	0.051; 0.037	0.085; 0.108
	(2,3-DMTTeA)$_5$AsF$_6$	(2,3-DMTTeA)$_2$Br
Formula	$C_8H_5As_{0.10}F_{0.60}Te_2$	$C_4H_{2.50}Br_{0.12}Te$
Formula mass	375.22	188.15
Crystal color, habit	black, needle	black, needle
Crystal system	monoclinic	tetragonal
a [Å]	4.155(2)	18.655(2)
b [Å]	19.898(3)	
c [Å]	11.572(7)	5.438(3)
β [°]	94.85(9)	
V [Å^3]	953.3(6)	1892(1)
Space group	$P2_1/a$ (#14)	$P4_2/ncm$ (#138)
Z	4	16
D_{calcd} [g cm^{-3}]	2.614	2.641
μ(Mo-K_α) [cm^{-1}]	64.07	71.54
Diffractometer	Rigaku AFC5R	Rigaku AFC5R
Radiation	Mo-K_α (λ = 0.71069 Å)	Mo-K_α (λ = 0.71069 Å)
Temperature [K]	296	296
Measured reflections	total: 3201, unique: 2853	total: 1313
Structure solution	Direct methods (SIR92)	Direct methods (SIR92)
Refinement	Full-matrix least-squares	Full-matrix least-squares
No. observations	1400 [I>3.00$\sigma(I)$]	578 [I>3.00$\sigma(I)$]
No. variables	109	56
Residuals: R;[a] R_w[b]	0.067; 0.082	0.095; 0.119

[a] $R = \Sigma||F_o| - |F_c||/\Sigma|F_c|$. [b] $R_w = [\Sigma\omega(|F_o| - |F_c|)^2/\Sigma\omega F_o^2]^{1/2}$.

Table 6. Crystallographic data of the TMTTeN salts.

	(TMTTeN)$_2$Ag(CN)$_2$	(TMTTeN)$_2$Au(CN)$_2$
Formula	$C_{3.5}H_3Ag_{0.12}Te$	$C_{3.5}H_3Au_{0.12}Te$
Formula mass	185.61	196.30
Crystal color, habit	black, needle	black, needle
Crystal system	tetragonal	tetragonal
a [Å]	18.2911(9)	18.322(1)
c [Å]	5.352(1)	5.350(3)
V [Å^3]	1790.5(4)	1795.9(9)
Space group	$P4_2/ncm$ (#138)	$P4_2/ncm$ (#138)
Z	16	16
D_{calcd} [g cm^{-3}]	2.754	2.904
μ(Mo-K_α) [cm^{-1}]	69.46	103.33
Diffractometer	Rigaku AFC7R	Rigaku AFC7R
Radiation	Mo-K_α (λ = 0.71069 Å)	Mo-K_α (λ = 0.71069 Å)
Temperature [K]	296	296
Measured reflections	total: 1582	total: 1586
Structure solution	Direct methods (SHELXS86)	Direct methods (SHELXS86)
Refinement	Full-matrix least-squares	Full-matrix least-squares
No. observations	927 [I>3.00$\sigma(I)$]	947 [I>3.00$\sigma(I)$]
No. variables	55	48
Residuals: R;[a] R_w[b]	0.035; 0.034	0.042; 0.044
	TMTTeN(SCN)$_{0.88}$	TMTTeN(ClO$_4$)$_{0.88}$
Formula	$C_{7.44}H_6NO_{0.44}S_{0.44}Te_2$	$C_{3.50}H_3Cl_{0.22}Te$
Formula mass	370.88	180.46
Crystal color, habit	black, prismatic	black, needle
Crystal system	monoclinic	tetragonal
a [Å]	5.419(3)	20.660(2)
b [Å]	17.493(2)	
c [Å]	8.941(2)	4.019(2)
β [°]	94.77(3)	
V [Å^3]	844.7(5)	1715(1)
Space group	$P2_1/a$ (#14)	$P4_2/ncm$ (#138)
Z	4	16
$D_{calcd.}$ [g cm^{-3}]	2.916	2.795
μ(Mo-K_α) [cm^{-1}]	69.40	68.58
Diffractometer	Rigaku AFC5R	Rigaku AFC7R
Radiation	Mo-K_α (λ = 0.71069 Å)	Mo-K_α (λ = 0.71069 Å)
Temperature [K]	296	296
Measured reflections	total: 2215, unique: 2013	total: 1534
Structure solution	Patterson methods (DIRDIF92 PATTY)	Direct methods (SHELXS86)
Refinement	Full-matrix least-squares	Full-matrix least-squares
No. observations	1223 [I>3.00$\sigma(I)$]	641 [I>3.00$\sigma(I)$]
No. variables	101	48
Residuals: R;[a] R_w[b]	0.035; 0.034	0.055; 0.068
	TMTTeN(AsF$_6$)$_{0.7}$	
Formula	$C_7H_6As_{0.35}F_{1.50}Te_2$	
Formula mass	400.04	
Crystal color, habit	black, needle	
Crystal system	tetragonal	
a [Å]	18.373(2)	
c [Å]	5.3236(9)	
V [Å^3]	1797.15	
Space group	P-42$_1m$ (#14)	
Z	8	
$D_{calcd.}$ [g cm^{-3}]	2.957	
μ(Mo-K_α) [cm^{-1}]	77.29	
Diffractometer	R-AXIS IV	
Radiation	Mo-K_α (λ = 0.71070 Å)	
Temperature [K]	296	
Measured reflections	total: 974	
Structure solution	Direct methods (SHELXS86)	
Refinement	Full-matrix least-squares	
No. observations	845 [I>3.00$\sigma(I)$]	
No. variables	111	
Residuals: R;[a] R_w[b]	0.072; 0.073	

[a] $R = \Sigma||F_o| - |F_c||/\Sigma|F_c|$. [b] $R_w = [\Sigma\omega(|F_o| - |F_c|)^2/\Sigma\omega F_o^2]^{1/2}$.

Ltd.). Data were accumulated for 100 s with time constants of 12 μs. Data collections and analyses were controlled by the Delta Class Analyzer (Kevex).

Magnetic Susceptibility Measurement: The magnetic susceptibilities were measured at a field of 30 kOe in the temperature range from 300 to 2 K using a Quantum Design MPMS-7 SQUID magnetometer. The samples were wrapped with clean aluminum foil whose magnetic susceptibility was separately measured and subtracted. The data were corrected for the diamagnetic contribution estimated from Pascal's constants, and the actual measurement of the neutral TMTTeN molecule [$\chi^{dia} = 7.47 \times 10^{-4}$ emu mol^{-1} for the $Ag(CN)_2^-$ salt and $\chi^{dia} = 3.63 \times 10^{-4}$ emu mol^{-1} for the SCN^- salt] and Curie impurities [0.05 mol-% for the $Ag(CN)_2^-$ salt and no subtraction of Curie impurities for the SCN^- salt].

Electrical Resistivity Measurement: The electrical resistivities were measured by a four-probe method along the donor stacking axis of the single crystals using Huso Electro Chemical System HECS 944C1 and/or HECS 944C Multi-channel 4-terminal conductometer. Electrical contacts were achieved with gold wires (Ø 0.015 mm) and gold paste.

Molecular Orbital (MO) and Band Structure Calculations: In order to use the simple extended Hückel type tight-binding band calculation for the molecular conductors based on *peri*-ditellurium-bridged polyacene donor molecules, reliable determination of the highest occupied molecular orbital (HOMO), from which a conduction band is formed, had to be made beforehand. The ab initio MO calculations of TMTTeN were performed by replacing the methyl groups with hydrogen atoms using Gaussian 94[28] on a Hewlett–Packard workstation (Apollo 9000 series model 735) at the Research Centre for Spectrochemistry of the University of Tokyo. The Huzinaga-Dunning double zeta basis set was used.[29] The Los Alamos effective core potential plus double zeta basis set (LanL2DZ) was used for tellurium atoms.[30]

The overlap integrals, band structures, and Fermi surfaces were calculated by a tight-binding method based on the extend Hückel approximation. Slater-type atomic orbitals were used for the calculation of MOs. The parameters for tellurium atoms were determined on the basis of the ab initio MO calculations and crystallographic analyses discussed before in this paper. The exponent ζ and the ionization potential (eV) were: Te 5s, 2.33, –17.41; Te 5p, 2.01, –8.98; Te 5d, 1.64, –4.76; C 2s, 1.625, –21.4; C 2p, 1.625, –11.4; H 1s, 1.0, –13.6. In the case of 2,3-DMTTeA salts, overlap integrals were calculated by using the coordinates of only one side of two conformations of the disordered molecule.

Acknowledgments

This work was supported by a Grand-in-Aid for Scientific Research on Priority Areas (No. 10149103 "Physical Properties of Solid-state Metal-assembled Complexes") from the Ministry of Education, Science, Sport and Culture, Japan.

[1] a) J. M. Williams, J. R. Ferraro, R. J. Thorn, K. D. Carlson, U. Geiser, H. H. Wang, A. M. Kini, M.-H. Whangbo, *Organic Superconductors (Including Fullerenes)*, Prentice Hall, New Jersey, **1992**; b) T. Ishiguro, K. Yamaji, G. Saito, *Organic Superconductors*, 2nd ed., Springer-Verlag, Berlin, Heidelberg, **1998**.

[2] a) A. Kobayashi, Y. Sasaki, R. Kato, H. Kobayashi, *Chem. Lett.* **1986**, 387–390; b) D. O. Cowan, A. Kini in *The Chemistry of Organic Selenium and Tellurium Compounds* (Ed.: S. Patai), John Wiley & Sons, London, **1987**, vol. 2, pp. 463–494; c) D. O. Cowan, R. McCullough, A. Bailey, K. A. Lerstrup, D. Talham, D. Herr, M. Mays, *Phosphorus Sulfur Silicon Relat. Elem.* **1992**, *67*, 277–294.

[3] R. D. McCullough, G. B. Kok, K. A. Lerstrup, D. O. Cowan, *J. Am. Chem. Soc.* **1987**, *109*, 4115–4116.

[4] E. Aharon-Shalom, J. Y. Becker, J. Bernstein, S. Bittner, S. Shaik, *Tetrahedron Lett.* **1985**, *26*, 2783–2786.

[5] a) K. Kikuchi, K. Yakushi, H. Kuroda, I. Ikemoto, K. Kobayashi, M. Honda, C. Katayama, J. Tanaka, *Chem. Lett.* **1985**, 419–422; b) Z. S. Li, S. Matsuzaki, R. Kato, H. Kobayashi, A. Kobayashi, M. Sano, *Chem. Lett.* **1986**, 1105–1108.

[6] G. Saito, S.-S. Pac, O. O. Drozdova, *Synth. Met.* **2001**, *120*, 667–670.

[7] D. O. Cowan, M. D. Mays, T. J. Kistenmacher, T. O. Poehler, M. A. Beno, A. M. Kini, J. M. Williams, Y. K. Kwok, K. D. Carlson, L. Xiao, J. J. Novoa, M.-H. Whangbo, *Mol. Cryst. Liq. Cryst.* **1990**, *181*, 43–58.

[8] a) M. A. Il'ina, E. S. Itskevich, *JETP Lett.* **1971**, *13*, 15–18; b) I. V. Berman, Z. I. Bynzarov, Y. P. Kurkin, *Sov. Phys. Solid State* **1973**, *14*, 2192–2194; c) M. A. Il'ina, E. S. Itskevich, *Sov. Phys. Solid State* **1976**, *17*, 2266–2267.

[9] a) E. N. Yakovlev, G. N. Stepanov, Y. A. Timofeev, B. V. Vinogradov, *JETP Lett.* **1978**, *28*, 340–342; b) V. V. Struzhkin, R. J. Hamley, H.-K. Mao, Y. A. Timofeev, *Nature* **1997**, *390*, 382–384.

[10] a) J. Witting, *Phys. Rev. Lett.* **1965**, *15*, 159–159; b) A. R. Moodenbaugh, C. T. Wu, R. Viswanathan, *Solid State Commun.* **1973**, *13*, 1413–1416.

[11] a) F. P. Bundy, K. J. Dunn, *Phys. Rev. B* **1980**, *22*, 3157–3164; b) Y. Akahama, M. Kobayashi, H. Kawamura, *Solid State Commun.* **1992**, *84*, 803–806.

[12] D. J. Sandman, J. C. Stark, B. M. Foxman, *Organometallics* **1982**, *1*, 739–742.

[13] D. J. Sandman, J. C. Stark, G. P. Hamill, W. A. Burke, B. M. Foxman, *Mol. Cryst. Liq. Cryst.* **1982**, *86*, 1819–1825.

[14] a) D. J. Sandman, J. C. Stark, M. Rubner, R. A. Acampora, L. A. Samuelson, B. M. Foxman, *Mol. Cryst. Liq. Cryst.* **1983**, *93*, 293–305; b) R. Kato, H. Kobayashi, A. Kobayashi, *Physica B+C* **1986**, *143*, 304–306.

[15] a) K. Takimiya, Y. Aso, T. Otsubo, F. Ogura, *Bull. Chem. Soc. Jpn.* **1991**, *64*, 2091–2102; b) For the sulfur and the selenium isologues of 2,3-DMTTeA, see: K. Takimiya, A. Ohnishi, Y. Aso, T. Otsubo, F. Ogura, K. Kawabata, K. Tanaka, M. Mizutani, *Bull. Chem. Soc. Jpn.* **1994**, *67*, 766–772.

[16] T. Otsubo, N. Sukenobe, Y. Aso, F. Ogura, *Synth. Met.* **1988**, *27*, B509–B514. Refs.[17–19] are preliminary communications.

[17] M. Nakata, A. Kobayashi, T. Saito, H. Kobayashi, K. Takimiya, T. Otsubo, F. Ogura, *J. Chem. Soc. Chem. Commun.* **1997**, 593–594.

[18] a) E. Arai, H. Fujiwara, H. Kobayashi, A. Kobayashi, K. Takimiya, T. Otsubo, F. Ogura, *Inorg. Chem.* **1998**, *37*, 2850–2851; b) A. Kobayashi, M. Nakata, E. Arai, H. Fujiwara, H. Kobayashi, K. Takimiya, T. Otsubo, F. Ogura, *Synth. Met.* **1999**, *103*, 1865–1868.

[19] E. Ojima, B. Z. Narymbetov, H. Fujiwara, H. Kobayashi, A. Kobayashi, K. Takimiya, T. Otsubo, F. Ogura, *Chem. Lett.* **1999**, 845–846.

[20] For example, a) T. Mori, A. Kobayashi, Y. Sasaki, H. Kobayashi, *Chem. Lett.* **1982**, 1923–1926; b) H. Kobayashi, R. Kato, A. Kobayashi, *Synth. Met.* **1997**, *19*, 623–628; c) A. Kobayashi, H. Kim, Y. Sasaki, H. Kobayashi, *Solid State Commun.* **1987**, *62*, 57–64.

[21] For example, a) K. Oshima, T. Mori, H. Inokuchi, H. Urayama, H. Yamochi, G. Saito, *Phys. Rev. B* **1988**, *38*, 938–941; b) W. Kang, G. Montambaux, J. R. Cooper, D. Jérome, P. Batail, C. Lenoir, *Phys. Rev. Lett.* **1989**, *62*, 2559–2562; c) K. Kajita, Y. Nishio, T. Takahashi, R. Kato, H. Kobayashi, W. Sasaki, A. Kobayashi, Y. Iye, *Solid State Commun.* **1989**, *70*, 1189–1193.

[22] R. P. Shibaeva, V. F. Kaminskii, *Sov. Phys. Crystallogr. Engl. Transl.* **1978**, *23*, 669–672.

[23] a) I. F. Shchegolev, E. B. Yagubskii in *Extended Linear Chain Compounds* (Ed.: J. S. Miller), Plenum Press, New York, **1982**, vol. 2, pp. 385–434; b) R. P. Shibaeva in *Extended Linear Chain Compounds* (Ed.: J. S. Miller), Plenum Press, New York, **1982**, vol. 2, pp. 435–467.
[24] R. P. Shibaeva, V. F. Kaminskii, A. I. Kotov, E. B. Yagubskii, M. L. Khidekel, *Kristallografiya* **1979**, *24*, 271–275.
[25] a) N. Toyota, T. Sasaki, Y. Watanabe, *Physica C* **1991**, *178*, 339–344; b) A. Kawamoto, K. Miyagawa, Y. Nakazawa, K. Kanoda, *Phys. Rev. Lett.* **1995**, *74*, 3455–3458.
[26] The width of the donor band of (TXF)(TCNQ) (X = S, Se, and Te) has been reported to be 0.85 eV (X = S), 1.52 (X = Se), and 2.49 (X = Te). E. D. Herr, M. D. Mays, R. D. McCullough, A. B. Bailey, D. O. Cowan, *J. Org. Chem.* **1996**, *61*, 7006–7011.
[27] *teXsan*, Crystal Structure Analysis Package, Molecular Structure Cooperation, **1985** and **1992**.
[28] M. J. Furisch, G. W. Trucks, H. B. Schlegel, P. M. W. Gill, B. G. Johnson, M. A. Robb, J. R. Cheeseman, T. Keith, G. A. Petersson, J. A. Montgomery, K. Raghavachari, M. A. Al-Laham, V. G. Zakrzewski, J. V. Ortiz, J. B. Foresman, J. Cioslowski, B. B. Stefanov, A. Nanayakkara, M. Challacombe, C. Y. Peng, P. Y. Ayala, W. Chen, M. W. Wong, J. L. Andres, E. S. Replogle, R. Gomperts, R. L. Martin, D. J. Fox, J. S. Binkley, D. J. Defrees, J. Baker, J. J. P. Stewart, M. Head-Gordon, C. Gonzalez, J. A. Pople, *Gaussian 94*, Gaussian, Inc., Pittsburgh, PA, **1995**.
[29] T. H. Dunning Jr., P. J. Hay in *Modern Theoretical Chemistry* (Ed.: H. F. Schaefer), Plenum, New York, **1976**, vol. III, pp. 1–28.
[30] W. R. Wadt, P. J. Hay, *J. Chem. Phys.* **1985**, *82*, 284–298.

Received: February 24, 2005
Published Online: July 20, 2005

